In vivo Electrophysiological Study of Induced Ventricular Tachycardia in Intact Rat Model of Chronic Ischemic Heart Failure

Kyle Weigand, Russell Witte, Talal Moukabary, Ike Chinyere, Jordan Lancaster, Mary Kaye Pierce, Steven Goldman*, and Elizabeth Juneman

Abstract*—*Objective: **The objective of this study was to define the clinical relevance of *in vivo* electrophysiologic (EP) studies in a rat model of chronic ischemic heart failure (CHF). *Methods:* Electrical activation sequences, voltage amplitudes, and monophasic action potentials (MAPs) were recorded from adult male Sprague–Dawley rats six weeks after left coronary artery ligation. Programmed electrical stimulation (PES) sequences were developed to induce sustained ventricular tachycardia (VT). The inducibility of sustained VT was defined by PES and the recorded tissue MAPs. *Results:* Rats in CHF were defined ($p < 0.05$) by elevated left ventricular (LV) end-diastolic pressure (5 $\pm$ 1 versus 18 $\pm$ 2 mmHg), decreased LV + d*P*/d*t* (7496 $\pm$ 225 versus 5502 $\pm$ 293 mmHg/ s), LV − d*P*/d*t* (7723 $\pm$ 208 versus 3819 $\pm$ 571 mmHg), LV ejection fraction (79 $\pm$ 3 versus 30 $\pm$ 3%), peak developed pressure (176 $\pm$ 4 versus 145 $\pm$ 9 mmHg), and prolonged time constant of LV relaxation Tau (18 $\pm$ 1 versus 29 $\pm$ 2 ms). The EP data showed decreased ($p < 0.05$) electrogram amplitude in border and infarct zones (Healthy zone (H): 8.7 $\pm$ 2.1 mV, Border zone (B): 5.3 $\pm$ 1.6 mV, and Infarct zone (I): 2.3 $\pm$ 1.2 mV), decreased MAP amplitude in the border zone (H: 14.0 $\pm$ 1.0 mV, B: 9.7 $\pm$ 0.5 mV), and increased repolarization heterogeneity in the border zone (H: 8.1 $\pm$ 1.5 ms, B: 20.2 $\pm$ 3.1 ms). With PES we induced sustained VT (>15 consecutive PVCs) in rats with CHF (10/14) versus Sham (0/8). *Conclusions:* These EP studies establish a clinically relevant protocol for studying genesis of VT in CHF. *Significance:* The *in vivo* rat model of CHF combined with EP analysis could be used to determine the arrhythmogenic potential of new treatments for CHF.**

***Index Terms*—Activation mapping, arrhythmias, chronic heart failure (CHF), electrophysiology (EP), ischemia, monophasic action potential (MAP), myocardial infarction (MI), rat model CHF, ventricular tachycardia (VT).**

I. Introduction

VENTRICULAR TACHYCARDIA (VT) and ventricular fibrillation (VF) are the most common causes of sudden cardiac death in patients with chronic heart failure (CHF). As the next generation of therapeutics for heart failure is developed, it is increasingly important to have reliable and clinically relevant preclinical models for characterizing the effects of drugs/treatments in the presence of myocardial infarction (MI) and CHF [1]–[3]. Furthermore, the complex and variable mechanisms of arrhythmias make predicting the electrical effects of new treatments in isolated cell preparations or perfused hearts difficult. For example, initial *in vitro* studies found cell transplantation to increase the likelihood of arrhythmias, whereas recent *in vivo* studies suggest the opposite [4]. *In vivo* animal models that allow for electrophysiological (EP) characterization of the effects of drugs, biologics, stem cells, and devices could define risk prior to the use in patients. In order to precisely define these changes, models for testing new therapies must be robust and clinically relevant in the realm of EP characterization. Tissue electrograms (for EP mapping) and monophasic action potential (MAP) recordings can help define the electrical integration of new treatments and potential associated arrhythmia risk [4]–[7]. To address this, we developed clinically relevant methods including EP mapping, MAP recording, and arrhythmia induction by programmed electrical stimulation (PES), permitting *in vivo* EP evaluation in an intact rat model of CHF.

Coronary artery ligation rat models of MI and CHF are also good models of ischemic cardiomyopathy that accurately predict clinical responses to drugs now used as standard therapy for CHF, such as angiotensin converting enzyme inhibitors and angiotensin receptor blockers [8], [9]. These studies accurately predicted the effects of these drugs on patients with CHF, not only in terms of improved left ventricular (LV) function, but also improved survival. These drugs are now the first line treatment for patients with heart failure. Therefore, understanding and performing EP testing in this model may be valuable

Manuscript received April 26, 2016; revised August 3, 2016; accepted August 22, 2016. Date of publication September 2, 2016; date of current version May 15, 2017. This work was supported in part by the WARMER Foundation, in part by the Sarver Heart Center, in part by the University of Arizona, in part by the Hansjörg Wyss Foundation, and in part by the Martin and Carol Reid Family Charitable Remainder Trust. *Asterisk indicates corresponding author.*

K. Weigand and R. Witte are with the Sarver Heart Center, and Biomedical Engineering, Optical Sciences, University of Arizona.

T. Moukabary is with the Carondelet Heart and Vascular Institute.

I. Chinyere and J. Lancaster are with the Sarver Heart Center, and Department of Physiology, University of Arizona.

M. K. Pierce was with the Sarver Heart Center, University of Arizona, and also with Cardiology and Medicine, Southern Arizona VA Health Care System.

*S. Goldman is with the Sarver Heart Center, University of Arizona, Tucson, AZ 85724 USA, and also with Cardiology and Medicine, Southern Arizona VA Health Care System, Tucson, AZ 85723 USA (e-mail: goldmans@shc.arizona.edu).

E. Juneman is the Sarver Heart Center, University of Arizona, and also with Cardiology and Medicine, Southern Arizona VA Health Care System.

Digital Object Identifier 10.1109/TBME.2016.2605578

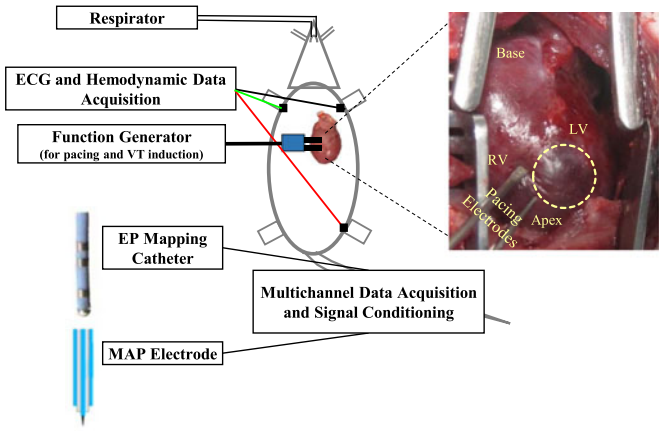

Fig. 1. (Left) General experimental setup showing a schematic of an open chest CHF rat. (Right) Photograph of open chest with pacing electrodes connected to the right ventricle (RV), showing the noninfarcted base of heart on top with the left ventricle (LV) and apex on the bottom. The enclosed yellow circle defines the infarcted area of the LV.

in preclinical translational research. In this study, we describe the same coronary artery ligation rat model of CHF with full EP characterization in the *in vivo* rat heart, including epicardial and MAP recording of healthy and infarcted tissue, as well as PES-induced arrhythmia with simultaneous MAP and electrocardiogram (ECG) recording. The methods generate EP datasets similar to what is observed in patients, including voltage amplitude decrease and conduction delay in infarcted tissue. Furthermore, MAP data allow for spatial localization of EP properties (such as repolarization heterogeneity) with respect to the underlying distribution of ischemic myocardium. We investigate these changes as they relate to the inducibility of arrhythmias in this model, and find that increased arrhythmia risk correlates strongly with viable myocardium which has abnormal action potential duration (APD), thus, indicating a physiological substrate for re-entry. Finally, MAP is recorded in the infarct border zone during the induction of VT, providing additional insight regarding mechanisms of arrhythmia and evolution of tissue in the region surrounding the scar.

II. Methods

A. Coronary Artery Ligation—CHF Induction

Rats in this study received humane care in compliance with IACUC-approved protocols at the University of Arizona. The rat coronary artery ligation technique is commonly used in our laboratory and is a well-established model to study the pathophysiology of CHF [2], [9]–[12]. In brief, male Sprague–Dawley rats were anesthetized with ketamine mixture and underwent a left thoracotomy. The heart was expressed from the thorax and a ligature placed around the proximal left coronary artery. Rats were recovered for six weeks to develop CHF.

B. Echocardiography

Transthoracic echocardiography was performed using a Vevo 2100 (Visual Sonics, ON, Canada) rodent echocardiography system and 25-MHz probe at 3 weeks and six weeks post-MI with views in the parasternal short axis and long axis, to evaluate the anterior, lateral, anterolateral, inferior, and posterior walls. Systolic displacement of the anterior wall and ejection fraction (EF) were obtained from two-dimensional (2-D) and M-mode measurements of myocardial wall thickness and LV dimensions [10]–[12]. Rats with EF $\leq$50% following permanent left coronary artery ligation at three weeks post-MI were enrolled in the study.

C. In Vivo Hemodynamic Measurements

Rats were anesthetized with an injection of Inactin (Sigma-Aldrich, St. Louis, MO), intubated, placed on a rodent ventilator and heated platform. A 3F pressure catheter (Millar, Houston, TX) was inserted through the carotid artery. The pressure sensor was equilibrated in 37 °C saline; LV and aortic pressures/heart rate were recorded and digitized at a rate of 1000 Hz to calculate LV dP/dt and the time constant (Tau) of LV relaxation using an AD Instruments Powerlab and Labchart system (AD Instruments, Colorado Springs, CO) [10]–[14]. Hemodynamic measurements were obtained at the end of the study, six weeks post-MI. A general system setup is shown in Fig. 1.

D. EP Mapping

Unipolar and bipolar recordings were obtained from multiple locations spanning the infarcted LV and surrounding tissue by a four-electrode EP catheter (Biosense Webster, Diamond Bar, CA). The two recording electrodes were used to map the epicardial surface of the ventricles and the resultant electrograms were used to generate voltage and activation maps (see Fig. 2). Pacing was performed at 2 $\times$ diastolic threshold. All waveforms were collected at a sampling rate of 2 kHz using a Biopac biosignal amplifier MP150 and MCE100C modules (Biopac Systems, Goleta, CA) and custom MATLAB software. Unipolar waveforms were high-pass filtered at 0.05 Hz and low-pass filtered at 100 Hz, and bipolar waveforms were high-pass filtered at 2.5 Hz and low-pass filtered at 500 Hz. All signals were notch filtered at 60 Hz to reduce contamination from electrical mains. Custom software developed in MATLAB analyzed waveforms for peak (absolute) voltage to define local voltage amplitude, and time to max $|dV/dt|$ from reference electrode in the right ventricle (RV), to define local activation time. Voltage and activation values were visualized using clinically relevant color maps and interpolated in 2-D to visualize ischemic tissue distribution and activation sequence. The thresholds were determined by a trained electrophysiologist (TM), who analyzed voltage mapping data and tissue gross appearance. We had to determine appropriate thresholds in rats with MIs and CHF, since this has not been reported previously in rats with epicardial recording. For reference and orientation, the maps were then overlaid on images of the heart in accordance with anatomical landmarks including the septum and the visible scar border (see Fig. 2). The surface ECG is used as a common point of reference. Since the electrograms are fractioned, the activation time is determined similar to the way it is done clinically in fractionated tissue. It is reviewed personally by the operator and compared to the surrounding tissue to choose the appropriate peak. If no clear local activation time was the point was rejected.

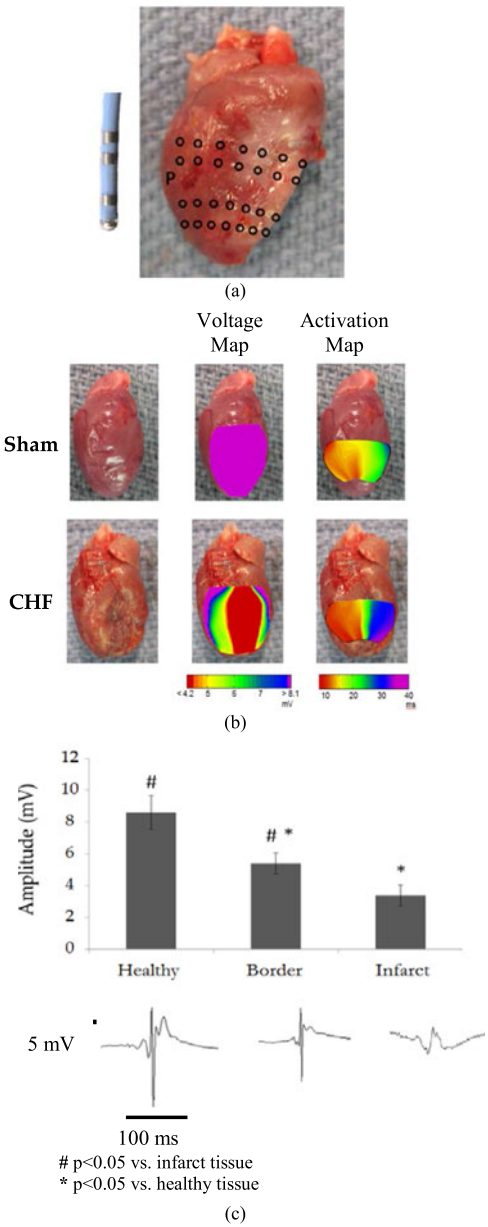

Fig. 2. EP mapping of the rat heart *in situ*. (a) recordings taken with quadrupolar catheter. Circles indicate 28 approximate recording locations spanning the LV, and "P" indicates pacing location for activation mapping. (b) EP mapping results for sham and CHF groups. Voltage map for normal heart shows all healthy tissue as expected. Voltage map for MI heart shows significant scarring with visible border zone. Sham activation map shows uniform conduction; CHF activation map shows significant delay in scarred region. (c) Three representative recordings from each tissue zone from each animal were compiled for quantifying voltage amplitude changes. Example electrogram shown below each tissue type. Significant changes in voltage amplitude observed for each zone (indicated by #, *).

E. MAP Recording

MAPs were recorded using a concentric bipolar electrode (World Precision Instruments, Sarasota, FL) at a sampling rate of 2 kHz using a Biopac biosignal amplifier and custom MATLAB software. The electrode was held in place with slight pressure applied to the LV epicardium. The electrode was not fixed or sutured; however, the pressure on the electrode ensured proper positioning during the beating of the heart. A motion artifact was occasionally observed resulting in unstable baseline, and these recordings were excluded from analysis. MAP recordings were obtained from multiple locations in healthy tissue and border tissue zones. Border tissue zone was identified visually and verified with associated voltage maps. A minimum of three recordings with stable baseline and consistent beat-to-beat morphology were chosen from each zone for subsequent analysis performed in MATLAB. Feature extraction included identification of MAP upstroke defined by max dV/dt, baseline, amplitude, and duration at 50%, 75%, and 90% repolarization. Repolarization heterogeneity was defined as the largest difference between measured MAPD_{90} between locations within each zone, as previously defined in other studies [13].

F. VT Induction

A protocol for PES was developed for studies in rats in accordance with the Lambeth conventions and using a modified version of the MUSTT Protocol for our studies [3], [4], [15]. Rats were paced from a healthy tissue in the RV at twice diastolic threshold for a drive-train of eight beats at a cycle length of S1–S1 = 160 ms, followed by up to two extra stimuli (S2, S3). S1–S2 and S2–S3 coupling intervals were decreased by 5 ms on each attempt until loss of capture. The effective refractory period (ERP) was defined as the longest S1–S2 interval with unsuccessful capture on S2. The second extra stimulus (S3) was not added until all S2's leading up to the ERP were delivered. The procedure ended when: 1) all pacing waveforms had been attempted through S3 loss of capture or 2) the animal exhibited long sustained VT resulting in compromised heart function. The MAP electrode was held in place at a location in the infarct border zone to record action potential changes during the induction of VT to capture localized EP data in addition to the surface ECG. Action potential recordings can help researchers distinguish between re-entrant mechanisms and abnormal impulse formation via the observation of afterdepolarizations. VT inducibility was summarized by the fraction of animals that exhibited induced sustained VT defined by VT lasting longer than 15 beats [16]–[20].

The activation sequence of VT was not mapped because we did not have the ability to record from multiple locations along the epicardial surface simultaneously. Our EP mapping was accomplished through a "stitched" mapping technique with waveforms collected at each site individually. In order to appropriately map VT, the VT needs to be sustained, monomorphic VT and last long enough to achieve the constituent recordings. In this model, even the longest VT events would not have allowed for this, given the limitations of our current technique.

G. Statistical Analysis

Data are expressed as mean ± SEM. Student's t-test for independent population means was used in analyzing significant changes ($p < 0.05$) with CHF (see Table I). Paired t-test was used for comparing MAP measurements taken from healthy and border tissue zones within the CHF group, and unpaired t-test

TABLE I

HEMODYNAMIC PARAMETERS REPRESENTATIVE OF LV FUNCTION ARE PRESENTED FOR SHAM ($N = 8$) AND CHF ($N = 14$) RATS. SIGNIFICANT CHANGES ($p < 0.05$) IN THE CHF INCLUDED: ELEVATED LV END-DIASTOLIC PRESSURE, DECREASED +LV dP/dT, DECREASED −LV dP/dT, DECREASED LV EJECTION FRACTION, DECREASED PEAK DEVELOPED PRESSURE, AND PROLONGED TIME CONSTANT OF LV RELAXATION/TAU

	HR (bpm)	EF%	EDP (mmHg)	SP (mmHg)	dP/dt(+) (mmHg)	dP/dt(−) (mmHg)	Tau (ms)	PDP (mmHg)
Sham	248 ± 7	79 ± 3	5 ± 1	135 ± 4	7496 ± 225	7723 ± 208	18 ± 1	176 ± 4
CHF	272 ± 6	$30 \pm 3^*$	$18 \pm 2^*$	$114 \pm 3^*$	$5502 \pm 293^*$	$3819 \pm 571^*$	$29 \pm 2^*$	$145 \pm 9^*$

Significant changes (p <0.05) in the CHF included: elevated LV end-diastolic pressure, decreased +LV dP/dt, decreased −LV dP/dt, decreased LV Ejection Fraction, decreased peak developed pressure, and prolonged time constant of LV relaxation/Tau.

was used for comparing MAP measurements between sham and CHF groups.

III. RESULTS

A. LV Function

Hemodynamic parameters representative of LV function are presented in Table I for Sham ($N = 8$) and CHF ($N = 14$) rats. Significant changes ($p < 0.05$) in the CHF included the following (see Table I): elevated LV end-diastolic pressure, decreased +LV dP/dt, decreased −LV dP/dt, decreased LV EF, decreased peak developed pressure, and prolonged time constant of LV relaxation/Tau. These data are consistent with a previous work in our laboratory documenting that this is a model of CHF [9]–[12].

B. EP Mapping

Unipolar electrogram amplitudes decreased in the border zone and further decreased in the infarct zone [Healthy tissue zone (H): 8.7 ± 2.1 mV, Border zone (B): 5.3 ± 1.6 mV, and Infarct zone (I): 2.3 ± 1.2 mV, see Fig. 2(c)]. Bipolar recordings taken from ischemic tissue exhibited increased fractionation, which occasionally made it difficult to determine activation time. Therefore, all waveforms were visually inspected to verify the deflection representative of local activation. The maps generated correlated well with visual observation of myocardial scar distribution with regard to both amplitude and activation time, and delayed activation through scar was consistently observed.

C. MAP Recording

MAP recordings showed expected morphology in healthy tissue (H) and in the border zone (B). Recordings taken from dense scar more closely resembled bipolar electrograms and were not used for analysis. MAP recordings in post-MI animals displayed a significant ($p < 0.05$) reduction in amplitude in the border zone (H: 14.0 ± 1.0 mV, B: 9.7 ± 0.5 mV), increased repolarization heterogeneity in the border zone (H: 8.1 ± 1.5 ms, B: 20.2 ± 3.1 ms), and decreased upstroke velocity (H: 0.88 ± 0.06 V/s, B: 0.65 ± 0.05 V/s) (see Fig. 2). Sample MAP recordings during sinus rhythm from each tissue zone are presented in Fig. 3.

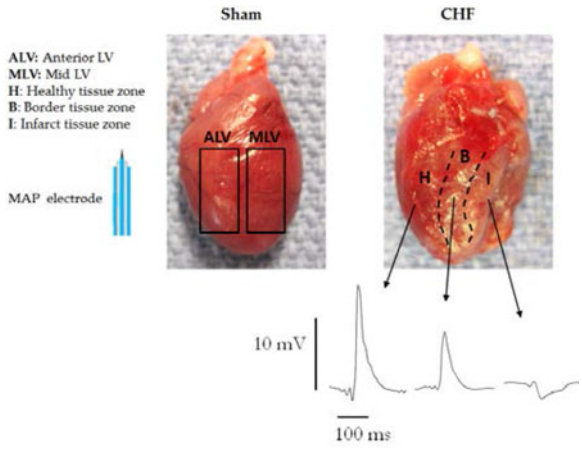

(a)

	Anterior LV	Mid LV	Anterior LV (Healthy)	Mid LV (Border)
MAP Amplitude (mV)	11.7±2.3	11.2±1.5	14.0±1.0	9.7±0.5*
$MAPD_{90}$ (ms)	63.9±1.9	63.9±1.7	61.7±2.6	65.3±2.8
$MAPD_{75}$ (ms)	42.6±1.2	45.3±1.3	42.7±1.9	47.8±2.2
$MAPD_{50}$ (ms)	25.2±2.0	26.3±1.6	26.9±1.2	30.3±1.4
Repol. Heterogeneity (ms)	9.2±2.5	8.7±1.8	8.1±1.5	20.2±3.1*^
Upstroke Velocity (V/s)	0.82±0.13	0.76±0.13	0.88±0.06	0.65±0.05*

*p<0.05 vs. CHF Healthy
^p<0.05 vs. Sham Mid LV

(b)

Fig 3. Summary of analysis for MAP recordings. (a) In CHF animals, border and healthy tissue zones were defined visually and verified using EP maps. In sham animals, border zone was defined by analogous locations on the LV, labeled as anterior LV (ALV) for sham healthy and mid LV (MLV) for sham border. Example waveforms from each tissue type shown below CHF heart; infarct zone shows significant MAP waveform degradation, excluding these recordings from analysis. (b) Table of values for MAP waveform analysis. Repolarization heterogeneity defined for each animal as the difference between the longest and the shortest measured 90% MAP duration ($MAPD_{90}$) in each zone. As expected, there is no change between healthy (ALV) and border (MLV) zone for sham animals. In CHF animals, amplitude of MAP decreases, repolarization heterogeneity increases, $MAPD_{75}$ and $MAPD_{50}$ increase, and upstroke velocity decreases in the border zone.

D. VT Induction With PES

Fourteen CHF rats and eight sham rats underwent PES for VT induction. Zero (out of eight) sham rats exhibited sustained VT (as defined as >15 consecutive beats), whereas ten of the fourteen (71.4%) CHF rats exhibited sustained VT (see Fig. 4). Two sham rats exhibited brief episodes of nonsustained VT.

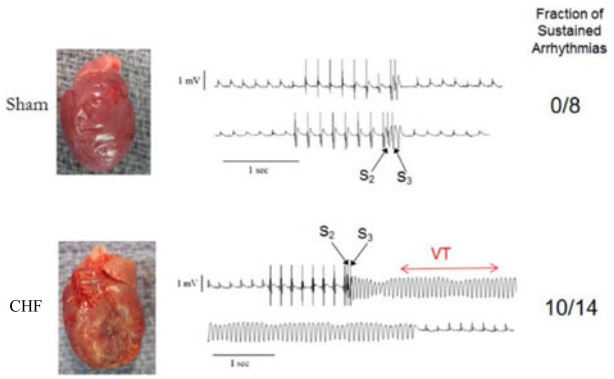

Fig. 4. Sample ECG waveforms for sham and CHF animals with fraction of inducible animals shown at right. Sustained monomorphic VT seen in CHF animal following S3 stimulus, whereas normal sinus rhythm returns following S3 in sham animal. Although 0% of the shams exhibited VT, 71.4% (10/14) of the CHF rats experienced VT.

MAP recording during the induction of VT enabled capture of local activity for studying mechanisms of different arrhythmia. This not only includes the classic re-entry but also triggered activity that was initiated by pacing. Triggered activity could explain the premature ventricular contractions and triggered VT that is occasionally observed clinically (see Fig. 5).

IV. Discussion

The goals of this study were to develop methods to 1) define and implement the induction of VT in rat coronary artery ligation model of ischemic CHF, and to 2) characterize EP changes at the tissue level using clinically relevant techniques *in vivo*. It is important to stress the clinical relevance of this model of CHF; first and foremost, we are studying an intact animal and not an isolated cell or perfused heart preparation. This is a model of stable CHF, as opposed to studying acute MI, where the genesis of ventricular arrhythmias is acute myocardial ischemia and the treatment is direct current cardioversion or institution of drug therapy such as lidocaine or amiodarone. In acute MI, the presence of ventricular arrhythmias does not predict mortality as closely as it does in CHF. In this model of CHF, ventricular remodeling has already taken place, with scar formation, thus, setting up the milieu for VT/VF that clearly predicts mortality. In this report, we define functional changes with hemodynamics and echocardiography documenting the presence of CHF in the rat *in vivo*, in addition to EP changes with EP mapping and MAP recordings, and risk of ventricular arrhythmia based on VT inducibility with PES. These data reflect what is seen clinically in CHF, suggesting that this model is a good representation of the pathophysiology of CHF.

To further clarify and compare our data to clinical data, VT in patients is defined as a ventricular rate greater than 100 beats/min and sustained VT is defined as lasting a minimum length of 30 s. Therefore, 30 s of VT at 100 beats/min would lead to a minimum of 50 consecutive ventricular beats for sustained VT in patients. In Fig. 4, the VT rate is approximately 840 beats/min. To achieve 50 consecutive ventricular contractions, the clinical minimum, 4 s would suffice, so we and other investigators chose 15 beats; this clearly exceeds the threshold for defining sustained VT in patients [16]–[20].

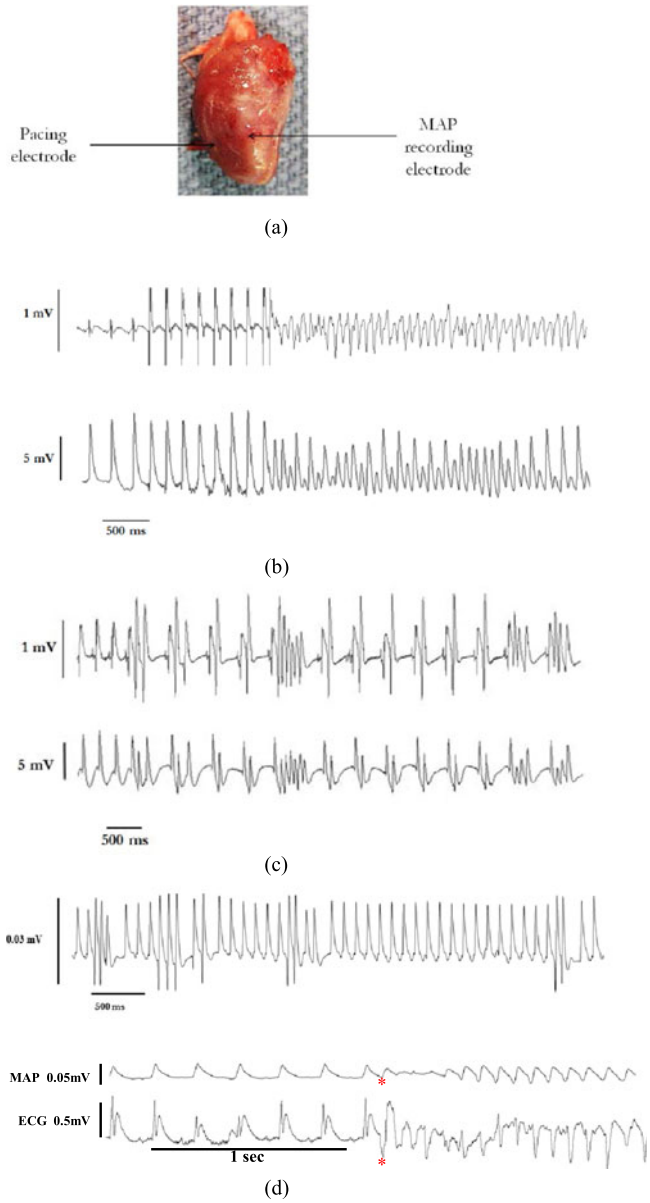

Fig. 5. During VT induction: (a) MAP electrode was held in place in the border zone where recording was viable. (b) Following PES, sustained polymorphic tachycardia is induced. MAP recording shows electrical alternans. (c) Three normal beats followed by spontaneous arrhythmia. Multiple DADs and nonsustained VT observed in both recordings. (d) Two normal beats followed by spontaneous arrhythmia with multiple DADs are observed throughout the MAP recording. Recording occurred prior to attempts of arrhythmia induction via PES. (e) Singular spontaneous delayed afterdepolarizations (*) followed by polymorphic VT.

A. EP Mapping

Color maps for voltage amplitude and activation sequence were defined using clinically-relevant color schemes and reflect the obtained values for healthy and scar tissue from the epicardium. Threshold voltage for healthy tissue (8.1 mV) was defined such that 90% of measurements taken from healthy epicardium were above the threshold, and similarly the value

for dense scar (4.2 mV) was defined such that 40% of measurements taken from the LVs of infarcted rats were below threshold. This allowed partially ischemic tissues to be distinguished from dense scar, and helped in defining border tissues while still visualizing the bulk of scar as a single color. The approach helps define threshold values for different tissue types in this model, producing color maps similar to what are used in the clinic to describe the distribution of ischemic tissue. To our knowledge, this is the first study to define epicardial voltage thresholds for healthy and ischemic cardiac tissues in the infarcted rat. The relatively large potentials from the epicardial surface of the rat may be due to the higher current densities in the thin wall of the rat heart compared to the human heart and has been observed by other groups.

B. Monophasic Action Potential

MAP recordings have been used to examine the electrophysiology of healthy and ischemic myocardial tissues. The MAP signals from dense myocardial scar in small animals do not display an expected morphology, and this is consistent with what was observed in this study. Therefore, it is assumed that MAP data can only compare healthy and partially ischemic tissues, as defined by EP maps and visual identification of tissue zones. We did not find a significant difference in overall APD between border zone (B) and healthy tissue (H) measurements (H: 61.7 ± 2.6 ms, B: 65.3 ± 2.8 ms). However, we did find a significant increase in repolarization heterogeneity between the two tissue types (H: 8.1 ± 1.5 ms, B: 20.2 ± 3.1 ms, $p < 0.007$). This APD heterogeneity specific to the border zone could be indicative of an additional arrhythmic EP substrate [13], [14], and agrees with the increased inducibility of VT in CHF animals. Recording action potentials prior to and during the induction of VT may provide additional information not detectable by the surface ECG. Analysis of these localized waveforms could help investigators distinguish the pathophysiology of the arrhythmia, and could therefore help explain changes in morphology based on known drug and arrhythmia mechanisms [21].

This information could help determine not only the effect of new agents on inducibility, but can also help localize changes at the tissue level that contribute to formation of an arrhythmic substrate. This has important implications in testing new treatments for CHF in preclinical models before agents are tested in humans. In this study, we report examples of MAP recording during onset of different arrhythmias to illustrate the potential value and relevance of the technique for describing delayed afterdepolarizations (DADs) (see Fig. 5), which are a consequence of the transient inward current that is related to abnormal calcium concentrations and/or handling. DADs are pro-arrhythmic because they can lead to rapid depolarization of surrounding tissue promoting re-entry. The finding of DADs is being proposed to suggest pro-arrthymic potential of drugs using organ on a chip technology [22].

C. Potential Future Uses of This Model

In addition to studying the effects of novel candidate drugs for treatment of CHF, this model could also be valuable for testing regenerative therapies for CHF. Previous studies transplanting skeletal myoblasts resulted in VT in patients with CHF [23] and this work stimulated attempts at antiarrhythmic engineering of skeletal myoblasts [24]. Investigators are also assessing arrhythmogenic risk of myocardial cell transplantation and mesenchymal stem cells in isolated Langendorff preparations. There is clearly a need to better understand the genesis and evolution of ventricular arrhythmias in intact animal models. For example, we have a particular interest in using induced pluripotent stem cells to treat CHF in patients in which very limited data are available [14], [25]–[29].

This study employed a novel platform with analysis software to study arrhythmias in rats with CHF. A clinical EP catheter was combined with a graphical user interface to perform EP studies in rats *in vivo*. The software was customized to accommodate the fast intrinsic heart rate in rats and, consequently, shorter stimulus drive trains (S_1, S_2, S_3) compared to humans. The program can be easily modified to accommodate small or large animal models, as well as different heart rates and pacing thresholds. Finally, in the future, a feedback algorithm could be employed to automatically determine the optimal parameters and threshold for inducing VT. A hybrid electrode array capable of stimulation and multichannel recording would facilitate closed-loop feedback for inducing and mapping arrhythmias.

D. Study Limitations

In humans, the size of postischemic scar is bigger on the endocardial surface. Although we performed epicardial mapping, the thickness of the ventricular wall is much less in the rat, so the transmural differences may be less. Although we defined the threshold voltage for healthy tissue as 8.1 mV and dense scar as 4.2 mV, there is no current standard in the rat for determining these cut-off thresholds, so our empirical method may be useful for other *in vivo* EP studies in rats for quantifying scar tissue. Because calcium handling in the rat heart is different than in humans, the genesis of arrhythmias may not perfectly predict this behavior in humans. Nonetheless, isolated perfused rat hearts have been used for many years to study the genesis of ventricular arrhythmias [30]–[32]. It is also possible to perform PES in intact rodents with a catheter introduced into the right ventricle [33]. Although these reports show that *ex vivo* rodent models can be used to study ventricular arrhythmias, we could not find reports using PES to induce sustained VT or MAPs to record arrhythmias in an intact rat model of ischemic CHF.

V. Conclusion

There is currently no effective clinical method to determine if a drug has the potential to induce VT in an animal model before it is tested on patients. We have presented EP studies with VT induction in an intact ischemic CHF rat model using modified clinical catheters and electrodes. The method we describe is a physiologic model where the electrical impulses can be characterized as they spread across native myocardium and predict the inducibility of sustained VT. The rat model and protocol could help determine the risk of arrhythmia from a new drug or treatment and offers an alternative to perfused rodent heart

preparations or costly large animal models commonly used for this purpose.

Acknowledgment

The author would like to thank M. Stansifer, Y. Qin, S. Daugherty, and N. LaHood for their technical assistance.

References

[1] F. Akar and R. Hajjar, "Gene therapies for arrhythmias in heart failure," *Eur. J. Physiol.*, vol. 466, pp. 1211–1217, 2014.
[2] C. Zaragoza *et al.*, "Review article animal models of cardiovascular diseases," *J. Biomed. Biotechnol.*, vol. 2011, pp. 1–13, 2011, Art. no. 497841 doi: 10.1155/2011/49784
[3] M. J. Curtis *et al.*, "The Lambeth conventions," *Pharmacol. Therapeutics*, vol. 139, no. 2, pp. 213–248, 2013.
[4] H. Cao *et al.*, "Electrical and mechanical strategies to enable cardiac repair and regeneration," *IEEE Rev. Biomed. Eng.*, vol. 8, pp. 114–124, 2015.
[5] F. J. Lee *et al.*, "Chaotic phase space differential algorithm for real-time detection of ventricular arrhythmias: application in animal models," in *Proc. IEEE Eng. Med. Biol. Soc. Conf.*, 2013, vol. 2013, pp. 2152–2155. doi: 10.1109/EMBC.2013.6609960
[6] L. Pattini *et al.*, "Dissecting heart failure through the multiscale approach of systems medicine," *IEEE Trans. Biomed. Eng.*, vol. 61, no. 5, pp. 1593–1603, May 2014.
[7] C. S. Henriquez. "A brief history of tissue models for cardiac electrophysiology," *IEEE Trans. Biomed. Eng.*, vol. 61, no. 5, pp. 1457–1465, May 2014. doi:10.1109/TBME.2014.2310515
[8] J. M. Pfeffer *et al.* "Influence of chronic captopril therapy on the infarcted left ventricle of the rat," *Circulation Res.*, vol. 57, pp. 84–87, 1985.
[9] J. J. Milavetz *et al.*, "Survival after myocardial infarction in rats: Comparison of captopril versus losartan," *J. Amer. College Cardiol.*, vol. 27, pp. 714–719, 1996.
[10] J. J. Lancaster *et al.*, "An electrically coupled tissue-engineered cardiomyocyte scaffold improves cardiac function in rats with chronic heart failure," *J. Heart Lung Transplantation*, vol. 33, pp. 438–445, 2014.
[11] J. J. Lancaster *et al.*, "Viable fibroblast matrix patch induces angiogenesis and increases myocardial blood flow in heart failure after myocardial infarction," *Tissue Eng., Part A*, vol. 16, no. 10, pp. 3065–3073, 2010.
[12] J. J. Lancaster *et al.*, "Induced pluripotent stem cell derived cardiomocyte scaffold improves electro-mechanical coupling and left ventricular function in rats with heart failure," *J. Cardiac Failure*, vol. 21, no. Suppl. 8, p. S92, 2015.
[13] M. Shrivastav *et al.*, "Following the beat of cardiac action potentials," *IEEE Potentials*, vol. 26, no. 3, pp. 19–25, 2007.
[14] S. Danik *et al.*, "Correlation of repolarization of ventricular monophasic action potential with ECG in the murine heart," *Amer. J. Physiol. Heart Circulatory Physiol.*, vol. 283, pp. H372–H381, 2007.
[15] A. Buxton *et al.*, "Prevention of sudden death in patients with coronary artery disease: The multicenter unsustained tachycardia trial (MUSTT)," *Prog. Cardiovascular Disease*, vol. 36, no. 3, pp. 215–226, 1993.
[16] M. Pahor *et al.*, "Programmed electrical stimulation-induced arrhythmias in isolated hearts from adult and senescent rats," *Can. J. Physiol. Pharmacol.*, vol. 67, pp. 472–476, 1988.
[17] T. Nguyen *et al.*, "Postinfarction survival and inducibility of ventricular arrhythmias in the spontaneously hypertensive rat," *Circulation*, vol. 98, pp. 2074–2080, 1998.
[18] T. M Lee *et al.*, "Effects of endothelin receptor antagonists on ventricular susceptibility in postinfarcted rats," *Amer. J. Physiol. Heart Circulatory Physiol.*, vol. 294, pp. H1871–H1879, 2008.
[19] T. M. Lee *et al.*, "Granulocyte colony-stimulating factor increases sympathetic reinnervation and the arrhythmogenic response to programmed electrical stimulation after myocardial infarction in rats." *Amer. J. Physiol. Heart Circulatory Physiol.*, vol. 297, pp. H512–H522, 2009.
[20] K. L. Jiao *et al.*, "Effects of valsartan on ventricular arrhythmia induced by programmed electrical stimulation in rats with myocardial infarction," *J. Cell. Mol. Med.*, vol. 6, pp. 1342–1351, 2012.
[21] J. N. Weiss *et al.*, "Early afterdepolarizations and cardiac arrhythmias," *Heart Rhythm*, vol. 7, pp. 1891–1899, 2010.
[22] M. Radisic. (2016, July). "Pathways to Cardiovascular Therapeutics," presentated at the AHA Basic Cardiovascular Sciences Scientific Session. [Talk]. Professionl.heart.org/bcvs 19, 2016.
[23] P. Menasche *et al.*, "Autologous skeletal myoblast transplantation for severe postinfarction left ventricular dysfunction," *J. Amer. College Cardiol.*, vol. 41, pp. 1078–1083, 2003.
[24] M. R. Abraham *et al.*, "Antiarrhythmic engineering of skeletal myoblasts for cardiac transplantation," *Circulation Res.*, vol. 97, pp. 159–167, 2005.
[25] L. Gepstein *et al.*, "*In vivo* assessment of the electrophysiological integration and arrhythmogenic risk of myocardial cell transplantation strategies," *Stem Cells*, vol. 28, no. 12, pp. 2151–2161, 2010. doi: 10.1002/stem.545.
[26] A. R. Costa *et al.*, "Optical mapping of cryoinjured rat myocardium grafted with mesenchymal stem cells," *Amer. J. Physiol. Heart Circulatory Physiol.*, vol. 302, no. 1, pp. H270–H277, 2012
[27] M. Kawamura *et al.*, "Feasibility, safety, and therapeutic efficacy of human induced pluripotent stem cell-derived cardiomyocyte sheets in a porcine ischemic cardiomyopathy model," *Circulation*, vol. 126, pp. S29–S37, 2012.
[28] M. Kawamura *et al.*, "Enhanced survival of transplanted human induced pluripotent stem cell-derived cardiomyocytes by the combination of cell sheets with the pedicled omental flap technique in a porcine heart," *Circulation*, vol. 128, no. 11 Suppl. 1, pp. S87–S94, 2013.
[29] S. G. Ong *et al.*, "Microfluidic single-cell analysis of transplanted human induced pluripotent stem cell-derived cardiomyocytes after acute myocardial infarction," *Circulation*, vol. 132, pp. 762–771, 2015.
[30] G. L. Aistrup *et al.*, "Pacing-induced h eterogeneities in intracellular Ca2 + signaling, cardiac alternans and ventricular arrhythmias in intact rat heart," *Circulation Res.*, vol. 99, pp. E65–E73, 2006.
[31] J. A. Wasserstrom *et al.*, "Characteristics of intracellular Ca^{2+} cycling in intact rat heart: a comparison of sex differences," *Amer. J. Physiol. Heart Circulatory Physiol.*, vol. 295, no. 5, pp. H1895–H1904, 2008.
[32] D. T. Nguyen *et al.*, "Pirfenidone mitigates left ventricular fibrosis and dysfunction after myocardial infarction and reduces arrhythmias," *Heart Rhythm*, vol. 10, pp. 1438–1445, 2010.
[33] N. Li and X. H. Wehrens, "Programmed electrical stimulation in mice," *J. Vis. Exp.*, vol. 39, 2010, Art. no. 1730.

Author' photograph and biography not available at the time of publication.